



Modeling and Simulation of Macroscopic Friction Coefficient of Brake Pair Considering Particle Flows and Interface Parameters

Shuaikang Liu¹ · Daogao Wei¹ · Bingzhan Zhang¹ · Liang Zhang¹ · Di Wu¹ · Wei Wang¹

Received: 6 July 2022 / Revised: 22 August 2022 / Accepted: 28 August 2022 / Published online: 7 October 2022
 © Krishtel eMaging Solutions Private Limited 2022, corrected publication 2022

Abstract

Purpose In this paper, a three-dimensional model of the disc brake pair considering the particle flows is firstly established, and the finite element simulation analysis of the brake pair friction performance is carried out to obtain the influence law of different braking parameters on the macroscopic friction coefficient and standard deviation.

Methods The macroscopic friction coefficient in the interface of brake pairs decreases from 0.4 to 0.152 with the increase of particle size, from 0.4 to 0.131 with the increase of particle density, and from 0.028 to 0.385 with the increase of rough peak radius of brake block. It was also found that the macroscopic friction coefficient gradually increased with the increase of the ratio of the rough peak radius of the brake block to the particle size, and the friction coefficient changed most drastically at its size ratio of about 1.5. By analyzing the change mechanism of the brake pair friction performance, it is believed that it is related to the embedding and deformation of the third body particles, and the simulation results are verified by bench tests.

Results Finally, a macroscopic friction coefficient model considering the third body particles and interface parameters were established, and the steady-state macroscopic friction coefficients under different braking parameters were calculated, and the R-square values of the models were above 0.9.

Conclusion This study can provide a reference for the braking pair friction algorithm of intelligent vehicles driving in sandy and dusty road conditions.

Keywords Disc brake pair · Finite element · Particle · Macroscopic friction coefficient · The friction model

List of Symbols

x_{pi}, y_{pi}	Particle output friction (N)	R_c	Rough peak radius of brake block (μm)
x_{pad}, y_{pad}	Brake block output friction (N)	V_r	Relative velocity (m/s)
F_f	Total friction (N)	COF	Friction coefficient
F_n	Load (N)	SD	Friction coefficient standard deviation
μ	Macroscopic friction coefficient	$\dot{\mu}$	The rate of change of macroscopic friction coefficient with time
σ	Standard deviation of macroscopic friction coefficient	var_i	Parameters affecting the friction characteristics of the braking pair
S	Brake pad area (m^2)	var_i	The rate of change of various characteristic parameters with time
P	Brake pressure (MPa)	f, f_1, f_2, \dots	Factors influencing the increase of friction coefficient
ω	Brake disc angular velocity (rad/s)	g, g_1, g_2, \dots	Factors influencing the reduction of friction coefficient
R_k	Particle size (μm)		
η_k	Particle density (n/m^2)		

✉ Daogao Wei
 weidaogao@hfut.edu.cn

¹ School of Automobile and Transportation Engineering, Hefei University of Technology, Hefei, Anhui, China

A_c	Actual contact area of brake block (m^2)
A_p	Nominal contact area of brake block (m^2)
$a, a_1, a_2, a_3, a_4, a_5, a_6,$ b, c, d, e, f, C_1	Undetermined coefficient
μ_{stab}	Steady-state macroscopic friction coefficient

Introduction

To clarify the origin of molecular friction and macroscopic friction, Sakuma et al. [1] performed density functional theory calculations on the mica surface, and the results confirmed that under sliding action, the potential roughness of mica is the origin of molecular friction, which depends on the normal stress and swipe direction. The discovered molecular friction mechanism can quantitatively explain the macroscopic friction of mica observed in the experiments. However, the automotive braking process is a very complex frictional dynamics phenomenon [2, 3], and its multi-frequency and multi-amplitude vibrations of the random dry friction force often lead to chattering, jittering and noise as well as braking friction instability during braking [4, 5]. Most of the available research results for this problem are based on the "disc-block" two-body coupled friction dynamics model. The concept of "three-body" originates from mechanical systems [6], and the third-body particles, consisting of abrasive and foreign particles generated by wear, are widely present in various mechanical systems such as machine tool guides, hydraulic turbine bearing friction pairs, bearing gear pairs, and robot joints. In the actual braking process, there are often particles from the external environment (such as sandy areas and sandy weather) or from their own wear [7–10], forming a three-body interface coupled frictional pair of "brake block–particle flows–brake disc", as shown in Fig. 1 [11]. The study of Godet [6] demonstrates that in the process of dry friction slipping, the friction performance is affected by the third body (particle flows), so it is inferred that the three-body coupling friction dynamics of "brake disc–particle flows–brake block" is different from the two-body coupling friction dynamics of "brake disc–brake block".

During friction, the flow of third-body particles from external sources or from the brake's own wear has an important effect on the friction characteristics. Y. Desplanque et al. [12] studied the coupling relationship between the heat migration of the braking system and the third-body particle flows formed by wear particles in the emergency braking of high-speed trains, and found that the interaction between the third-body particle flows and the radial heat migration in the

brake system affects the change of the friction coefficient of the braking pair. K.H. Cho et al. [13] took the brake block containing Zircon particles with different particle sizes of 1 μm , 6 μm , 75 μm and 150 μm as samples to study the influence of the third-body transfer film formed by Zircon particles generated by their wear on the friction coefficient of the three-system dynamic pair. The results showed that under braking conditions, the brake block containing Zircon particles with small particle size formed a third-body transfer film, which resulted in a large fluctuation of friction coefficient at the interface of the brake pair. M. K. Abdul Hamid et al. [14] investigated the effect of particle size from outside on the frictional dynamic characteristics of the three-body brake pair, and the results of a large number of bench tests showed that the friction coefficient of the three-body brake pair increases with decreasing particle size, and the effect of particle size on the fluctuation of the brake friction coefficient is more significant at high braking speeds.

There are also a number of scholars who have conducted finite element modeling and analysis for the mechanical behavior of dry contact sliding between brake disc and brake block. A. Belhocine et al. [15, 16]. performed numerical simulations for transient thermal analysis and static structural analysis using ANSYS software with a coupled thermal-structural method. It was found that in the presence of thermal effect, contact pressure of pad and overall, deformation of the brake disc are quite considerably prominent [17]. The literature [18] investigated the structural and mechanical behavior of a three-dimensional disk-pad model during braking under dry contact sliding conditions. It is shown that increasing the disc rotation speed decreases the equivalent Von Mises stresses and disc shears stress and results in an increase in the normal constraints of the disc and the friction pressures and stresses and the total deformation of the pads. Belhocine et al. [19] investigated the effect of Young's modulus variations of the disc brakes components on the squeal propensity using a detailed three-dimensional finite element model. The simulation result showed that instability of the disc brakes made it sensitive to Young's modulus variations of the disc brake components. But for the "brake block–particle flowsbrake disc" three-body friction contact simulation is less, currently for particulate matter more use is the discrete element method (DEM) and finite element method (FEM). Iordanoff et al. [20, 21] established a three-dimensional discrete element model to simulate the separation, contact flow and ejection processes of particles, and using discrete element theory, the mechanical interaction between particles was equated to the existence of connecting bonds between particles, and the breaking of the connecting bonds was manifested by the occurrence of particle detachment, flow and exclusion of friction surfaces. The results show that the number of dependent third bodies on

the contact surfaces increases as the strength of the connecting bonds between the third body particles increases. Hou et al. [22] established a parallel plate shear cell to simulate the shear motion of a parallel plate and observe the variation of relevant parameters, and divided the shear expansion process into three stages: plastic strain, macroscopic damage and particle reorganization, and the results showed that there were significant differences in the load distribution rate curves of the three stages.

The behavior of the third-body particle flows is special in that it is neither fluid nor solid, yet has both fluid and solid properties, and is time-varying, which often brings many uncertainties in the braking process, resulting in more complex frictional behavior of the braking pair. At present, for the frictional contact problem of the brake, the focus is only on the frictional contact of the two bodies, and the influence of the particle flows of the third body is overlooked. Due to the difficulty of the discrete element method in solving the multi-body contact of complex geometry and the deformation of granular materials, coupled with the limited experimental conditions, it is impossible to observe the braking interface in real time during the braking process. Therefore, this paper uses finite element software (ABAQUS). The main purpose is to numerically simulate the friction stress in the braking process, and obtain the influence of different braking parameters on the friction performance of the brake pair through a large number of simulation calculations. By analyzing the matching relationship between the rough peak of the brake block and the size of the third body particles, the influence of the ratio of the two on the macroscopic friction coefficient of the brake pair is derived, which provides a theoretical reference for the design and manufacture of the brake block and improves its service life. Finally, a macroscopic friction coefficient model containing particles affecting factors is established, which can provide a reference for the algorithm of the brake pair friction force of intelligent vehicles driving in sand and dust conditions, further optimize the stability of the automotive brake system and improve the safety and comfort of the whole vehicle.

The flow of the technical route in this paper is shown in Fig. 2:

Finite Element Modelling and Analysis

Modeling Assumptions

In this paper, a finite element method is used to simulate the frictional properties of a three-body disc brake pair. To improve the computational efficiency and to reduce the influence of unnecessary factors, these assumptions which are made while modeling the process are given below:

1. The brake disc, brake block and third body particles are all isotropic materials, that is, the mechanical properties of the medium at each point in the object and the properties in all directions are considered to be the same.
2. The ambient temperature is kept constant during the braking process, and the initial temperature of the system is 20 °C.
3. Wear of the friction material during the braking process is not considered.
4. During the braking process, all contacts within the friction system are adapted to Coulomb friction conditions.
5. The third body particles involved in the friction have the same particle size and are considered as an aggregate of materials with the properties of brake block materials, and all present spherical particles.

Three-Dimensional Modeling

The surface of the brake disc is smooth, the surface of the brake block has evenly distributed hemispherical rough peaks, and the third body particles are evenly distributed between the brake disc and the brake block. To simulate the effect of micron-level particles on the friction performance of the brake pair, the modeling requires an equivalent reduction in the size of the brake disc and the brake block. The brake disc radius is 3 mm, the brake block outer diameter is 2.5 mm, the inner diameter is 2 mm, and the particles are at micron level, as shown in Fig. 3.

Material Properties

In the model of this paper, the main friction component performance parameters are shown in Table 1 [23]. For material plasticity, a series of straight lines with given data points are used to approximate the smooth stress–strain curve of the material, so the more data points selected, the more realistic the nature of the simulated material is, and the data points for the plastic behavior of the steel material are shown in Table 2 [23], and the plastic behavior of the carbon fiber material is similar.

Meshing the Model

For the brake disc and the particle, the structure is relatively single and regular in shape, the free mesh and structural mesh division are used, respectively. For the brake block, the structure is more complex. It is first cut into multiple regular shaped parts, and then the seeds are placed to divide the mesh. The overall meshing effect is shown in Fig. 4. The whole assembly is divided into a total of 36,459 elements and 53,072 nodes. The mesh division of each component is shown in Table 3.

Analysis Step Setting

Combined with the characteristics of the particle flow process, this simulation uses the explicit analysis module (ABAQUS/Explicit), and the computational cost of solving complex nonlinear problems is significantly smaller than that of the Standard module, and there is no convergence problem. The simulation process sets two analysis steps, step1 time is set to 1×10^{-5} s for applying the normal load, step2 time is set to 1×10^{-2} s, the brake disc starts to rotate, and the whole braking process is simulated.

Constraint Conditions and Loads

According to the real situation when braking, the brake block only moves in the Z direction and the brake disc moves in a circular motion, so a fixed constraint is applied to the back of the brake block in both the X- and Y-axes. The center point of the brake disc is selected as the reference point, and the coupling constraint between the brake disc and the reference point is applied to drive the rotation of the brake disc by controlling the rotation of the reference point. The spherical particles are uniformly arranged in the brake disc and brake block gap, and the brake block and each particle are contacted with the brake disc using the contact pair algorithm for contact constraint, while the other surfaces in contact with each other use the general contact algorithm. For the tangential behavior of the contact property, the friction coefficient is defined as 0.4. The final 3D model is shown in Fig. 5.

Run Simulation

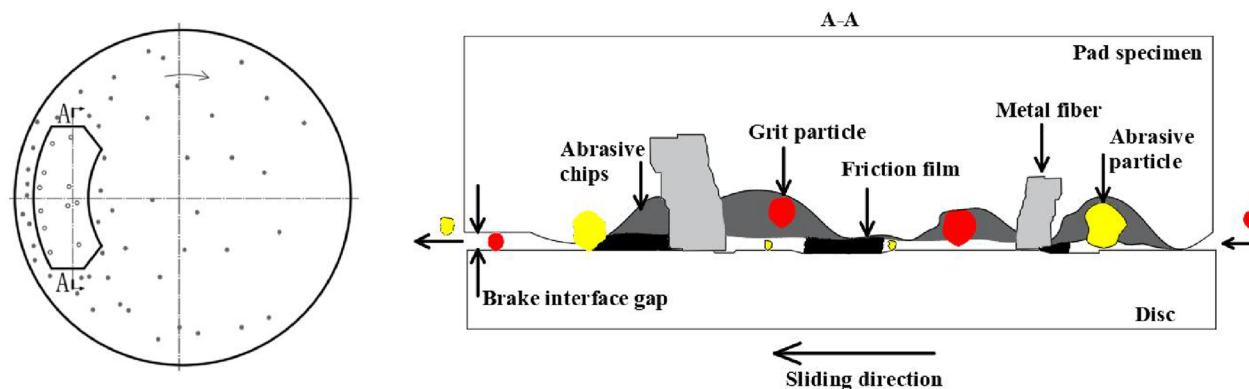
Submit the job and go to the result to see it after completion. The simulation motion process is shown in Fig. 6.

Data Processing

In the process of contact, the force of the brake disc by the particle flow can be divided into two parts: normal force and tangential force, where the force in the normal direction is the squeezing pressure between the particle body and the lower surface, and the force in the tangential direction is the resistance of the lower surface to obstruct the movement of the particle body, which is the friction force. Each particle and the brake block have frictional effect on the brake disc, so the friction force of the particles and the brake block on the brake disc is the total friction force, and not only the lateral friction force (X direction) should be considered, and also consider the longitudinal friction force (Y direction). Assuming that the friction forces in the X-direction and Y-direction of the i th particle output are x_{pi} and y_{pi} , respectively, and the friction forces of the brake block on the brake disc in the X-direction and Y-direction are x_{pad} and y_{pad} , respectively, the formula for the total friction force and the macroscopic friction coefficient is derived as follows:

$$F_f = \sqrt{\left(\sum_{i=1}^n \bar{x}_{pi} + x_{pad}\right)^2 + \left(\sum_{i=1}^n \bar{y}_{pi} + y_{pad}\right)^2}, \tag{1}$$

$$\mu = \frac{F_f}{F_n} = \frac{F_f}{PS}. \tag{2}$$



(a) Three-body brake pair with particle flows

(b) Three-body interface with particle flows

Fig. 1 Three-body interface coupling model of "brake block–particle flows–brake disc"

Results and Discussion of Finite Element Analysis

Influence of Fine Mesh

Table 4 shows the results of the numerical simulation of the mesh from coarse to fine, and it can be observed that the extreme value of the macroscopic friction coefficient decreases with the increase of the number of elements and nodes in favor of friction stability. Therefore, a finer grid division is chosen in this paper, with the total number of elements being 36,459 and the number of nodes being 53,072.

Influence of Brake Pressure

The braking pressures were set to 0.2, 0.3, 0.4, 0.5 and 0.6 MPa, respectively, and the macroscopic friction coefficients and standard deviations at different braking pressures were derived and plotted as the variation curves shown in Fig. 7. Other parameters: $R_k = 30 \mu\text{m}$, $R_c = 40 \mu\text{m}$, $\eta_k = 10/\text{m}^2$, and $\omega = 50 \text{ rad/s}$.

It can be seen from Fig. 7 that with the continuous increase of the braking pressure, the macroscopic friction coefficient of the braking pair interface increases from 0.136 to 0.205, and its standard deviation finally drops to 0.075 with the increase of the pressure, that is, the friction fluctuation becomes smaller.

Influence of Brake Disc Angular Velocity

The brake disc angular speed was set to 20, 30, 40, 50 and 60 rad/s, respectively, and the macroscopic friction coefficients and standard deviations were derived for different brake disc angular speeds, and the variation curves were plotted, as shown in Fig. 8. Other parameters: $R_k = 40 \mu\text{m}$, $R_c = 40 \mu\text{m}$, $\eta_k = 10/\text{m}^2$, and $P = 0.5 \text{ MPa}$.

It can be seen from Fig. 8 that with the continuous increase of the angular velocity of the brake disc, the macroscopic friction coefficient of the brake pair interface shows a decreasing trend, from 0.221 to 0.206, which is relatively gentle, and its standard deviation generally increases with the increase of the angular velocity, from 0.061 increases to 0.079, that is, the friction fluctuation becomes larger. Combined with Figs. 7 and 8, it can be seen that the influence degree of braking pressure and angular velocity on the macroscopic friction coefficient of the three-body braking pair is obviously different.

Influence of Particle Size

The particle sizes were set to 0, 10, 15, 20, 25, 30, 35, 40, 50 and 60 μm , respectively, and the macroscopic friction

coefficients and standard deviations were derived for different particle sizes, and the variation curves are plotted as shown in Fig. 9. Other parameters: $R_c = 40 \mu\text{m}$, $\eta_k = 10/\text{m}^2$, $P = 0.5 \text{ MPa}$, $\omega = 50 \text{ rad/s}$.

As can be seen from Fig. 9, the macroscopic friction coefficient tends to decrease as the particle size increases. In different particle size ranges, the rate of macroscopic friction coefficient decreases differently. In the interval of particle size 20–40 μm , the macroscopic friction coefficient decreases sharply, from 0.362 to 0.171, which is nearly linear. The standard deviation of the macroscopic friction coefficient has a trend of first increasing and then decreasing with the increase of particle size, that is, after the particle size exceeds 35 μm , the friction fluctuation begins to decrease.

Influence of Particle Density

The particle densities were set to 0, 8, 10, 16, 24, 32, 40, 50/ m^2 , respectively, and added uniformly in the brake block area to derive the macroscopic friction coefficients and standard deviations at different particle densities, and plotted the variation curves as shown in Fig. 10. Other parameters: $R_k = 30 \mu\text{m}$, $R_c = 40 \mu\text{m}$, $P = 0.5 \text{ MPa}$, $\omega = 50 \text{ rad/s}$.

It can be seen from Fig. 10 that with the increase of particle density, the macroscopic friction coefficient shows a decreasing trend, from 0.4 to 0.131, and the change is very obvious. Although the standard deviation has decreased in some intervals, the overall trend has increased, that is, the fluctuation has become larger.

Influence of Rough Peak Radius of Brake Block

The brake block rough peak radii were set to 0, 20, 30, 40, 50, 55, 60, 70 and 100 μm , respectively, and the macroscopic friction coefficients and standard deviations were derived for different brake block rough peak radii, and the variation curves were plotted as shown in Fig. 11. Other parameters: $R_k = 30 \mu\text{m}$, $\eta_k = 10/\text{m}^2$, $P = 0.5 \text{ MPa}$, $\omega = 50 \text{ rad/s}$.

It can be seen from Fig. 11 that with the increase of the radius of the roughness peak of the brake pad, the macroscopic friction coefficient shows an increasing trend. Similar to the particle size variation relationship, the friction coefficient increases at different rates in different roughness peak radius ranges. When the radius of the rough peak is in the range of 20–60 μm , the macroscopic friction coefficient increases sharply, from 0.105 to 0.348, in an approximately linear fashion. The standard deviation of the macroscopic friction coefficient increases first and then decreases with the increase of the asperity peak radius, that is, the fluctuation becomes smaller when the rough peak radius exceeds 55 μm . Combined with Figs. 9 and 11, it can be seen that the

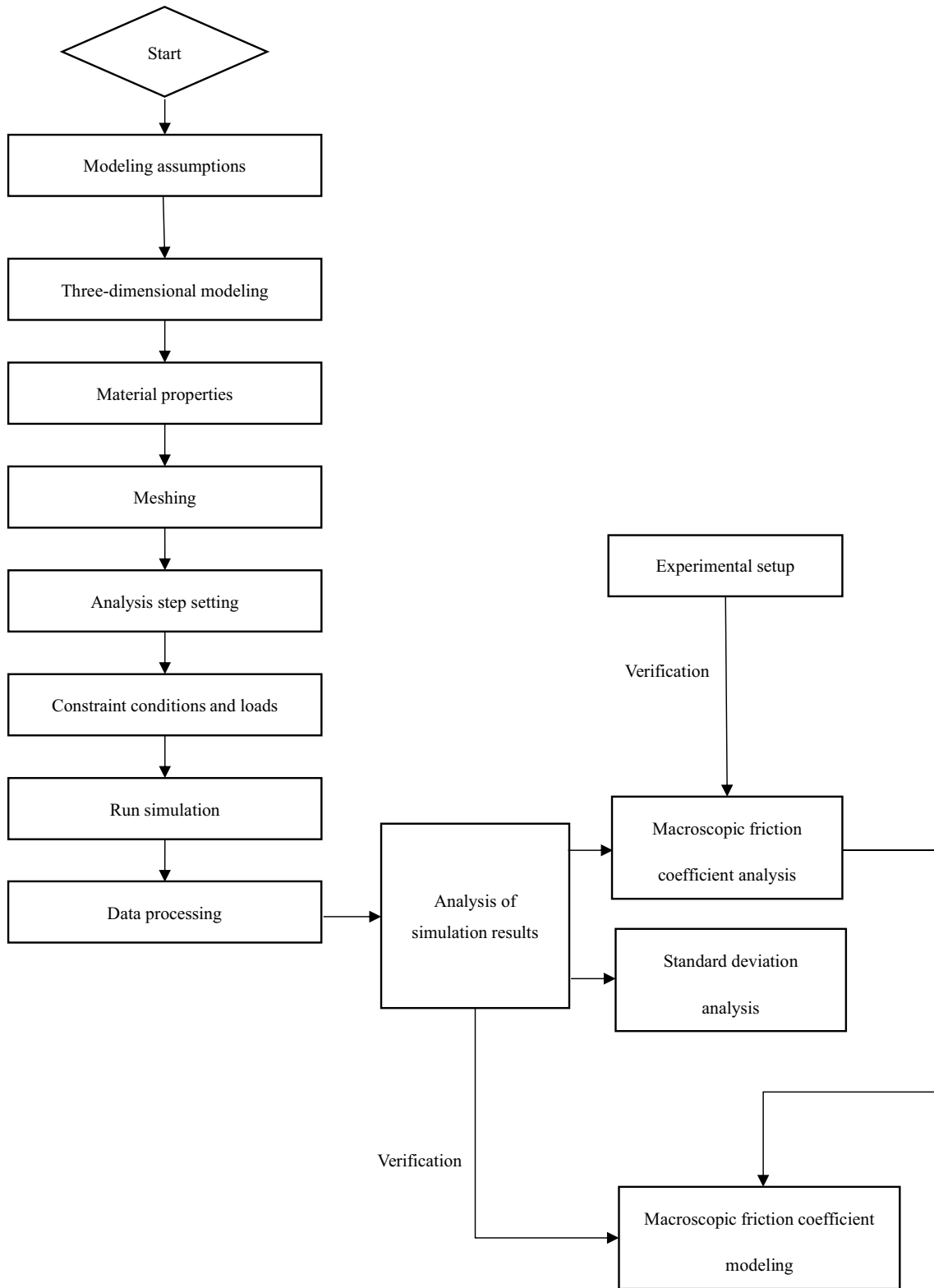


Fig. 2 Methodology of present study

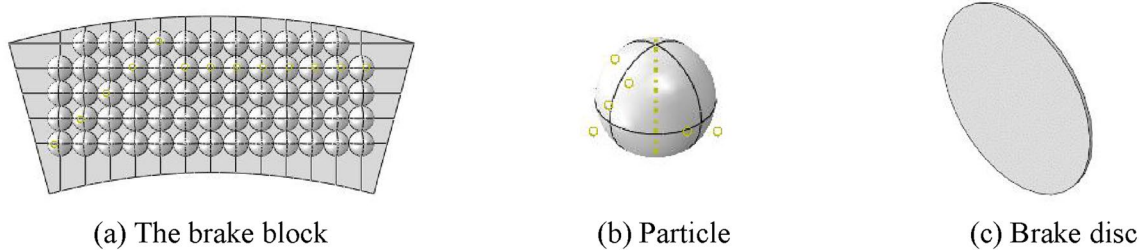


Fig. 3 Model of each friction part

Table 1 Performance parameters of friction parts

Material	Main ingredients	Density (g/cm ³)	Young's modulus (MPa)	Poisson's ratio
Brake disc	The steel material	7.8×10^{-9}	210,000	0.3
The brake block	Carbon fiber composite	1.5×10^{-9}	40,000	0.31
Particle	Carbon fiber composite	1.5×10^{-9}	40,000	0.31

macroscopic friction coefficient gradually increases with the increase of the ratio of brake block rough peak radius to particle size, and the macroscopic friction coefficient changes most drastically when its ratio is about 1.5, and changes gently in the other ratio intervals. Therefore, it is possible to provide theoretical reference for the design of the brake block from the matching relationship between the particle size and the radius of the rough peak of the brake block, and select the appropriate rough peak of the brake block to obtain the best braking performance.

The above simulation results are consistent with the overall trend of the results in the literature [14, 24, 25], especially the study in the literature [24] showed that the overall friction coefficient tends to decrease with the increase of the maximum (minimum) particle diameter and particle density, while the friction coefficient gradually increases with the increase of the root mean square value of the rough peak height.

Mechanistic Analysis

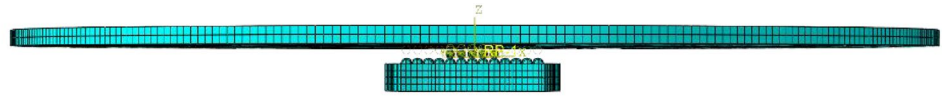
By simulating the influence of different braking parameters on the friction performance of the three-body brake pair, it is found that the macroscopic friction coefficient of the brake pairs and the fluctuation in the friction process is related to the deformation and embedding of the third-body particles, as shown in Fig. 12 (the brake disc was hidden during observation to clearly see the particle motion in the interface). The particles first undergo elastic deformation under the pressure of the brake block. After exceeding the elastic limit, they enter the yield stage and undergo plastic deformation. The particles after plastic deformation are not conducive to rolling friction in the three-body interface,

Table 2 Stress–strain in the plastic phase of steel materials

True stress (MPa)	Plastic strain	True stress (MPa)	Plastic strain
418	0	882	0.25
500	0.01581	908	0.35
605	0.02983	921	0.45
695	0.056	932	0.55
780	0.095	955	0.65
829	0.15	988	0.75

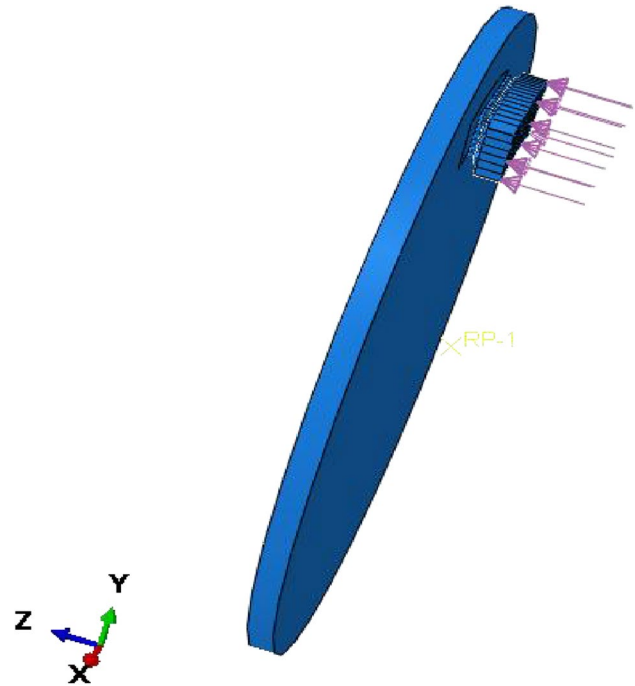
and the sliding friction component increases accordingly, making the ratio of interfacial rolling friction to sliding friction decreases, and the macroscopic friction coefficient increases. The deformed particles are very easy to fall into the gap between the rough peaks during the movement process, which reduces the number of third-body particles. At this time, the load on the remaining unembedded particles increases again, which intensifies the plastic deformation of the particles. Under repeated action, the interface tends to "brake disc–brake block" two-body friction, which increases the macroscopic friction coefficient again, so the embedding and deformation of the third body particles will increase the macroscopic friction coefficient. Particles in a limited space in the sharp rolling slip, particles and brake discs, particles and brake blocks and particles and particles between the rotation, collision, impact intensified, the friction is more violent, while the particles embedded will slow down this phenomenon, so that friction fluctuations are reduced.

The above braking parameters all affect the friction performance by changing the deformation and embedding of the particles, which in essence changes the ratio of the two-body

Fig. 4 Assembly model meshing**Table 3** Mesh division of each component

No.	Name	Mesh method	No. of elements	No. of nodes
1	Brake disc	Hexahedral	28,446	43,229
2	Particle	Hexahedral	1320	1611
3	Brake block	Hexahedral	6693	8232

area (direct contact area between two contact surfaces) and the three-body area (indirect contact area between two contact surfaces through a third body medium) in the contact area, thereby changing the actual contact area of the braking interface. Higher braking pressure increases the degree of particle deformation and increases the proportion of particles embedded in the rough crest gap of the brake block, both of which increase the macroscopic friction coefficient. The increase of the angular velocity of the brake disc will speed up the flow of the particles, but it is not easy to fall into the gap between the rough peaks, and the macroscopic friction coefficient decreases slowly. With the increase of particle size, it is more difficult for the particles to embed into the rough peak gap of the brake block. At the same time, the ability of the particles to carry pressure increases, and the particle deformation decreases, resulting in a gradual decrease in the macroscopic friction coefficient. As the density of particles in the brake interface increases, the more particles that fail to embed in the rough peak gap of the brake block, that is, the proportion of particles embedded decreases, and the composition of rolling friction increases. At the same time, the average load per particle is lower and the deformation is weaker, both of which lead to a smaller macroscopic friction coefficient. The larger the radius of the rough peak of the brake block, the easier the particles are embedded in the process of movement, the braking interface tends to "brake disc-brake pad" two-body friction, so the macroscopic friction coefficient increases and the fluctuation is small.

**Fig. 5** The final 3D model

Experimental Setup

Brake Pressure Test

This experiment uses the XD-MSM constant-speed friction tester provided by the Institute of Tribology of Hefei University of Technology to verify some of the above simulation results, as shown in Fig. 13a, b, which are the physical photos of the tester. The tester can be used to measure the friction coefficient and wear rate of brake linings and other friction materials for automobiles, and the experimental operation process is carried out with reference to GB5763-2008 standard. The test material is a resin-based friction plate, the size of 25 mm × 25 mm × 6 mm, the counterpart material is gray cast iron HT250, pearlite organization, the hardness of HB170~210 (GB976-67). To maintain the same

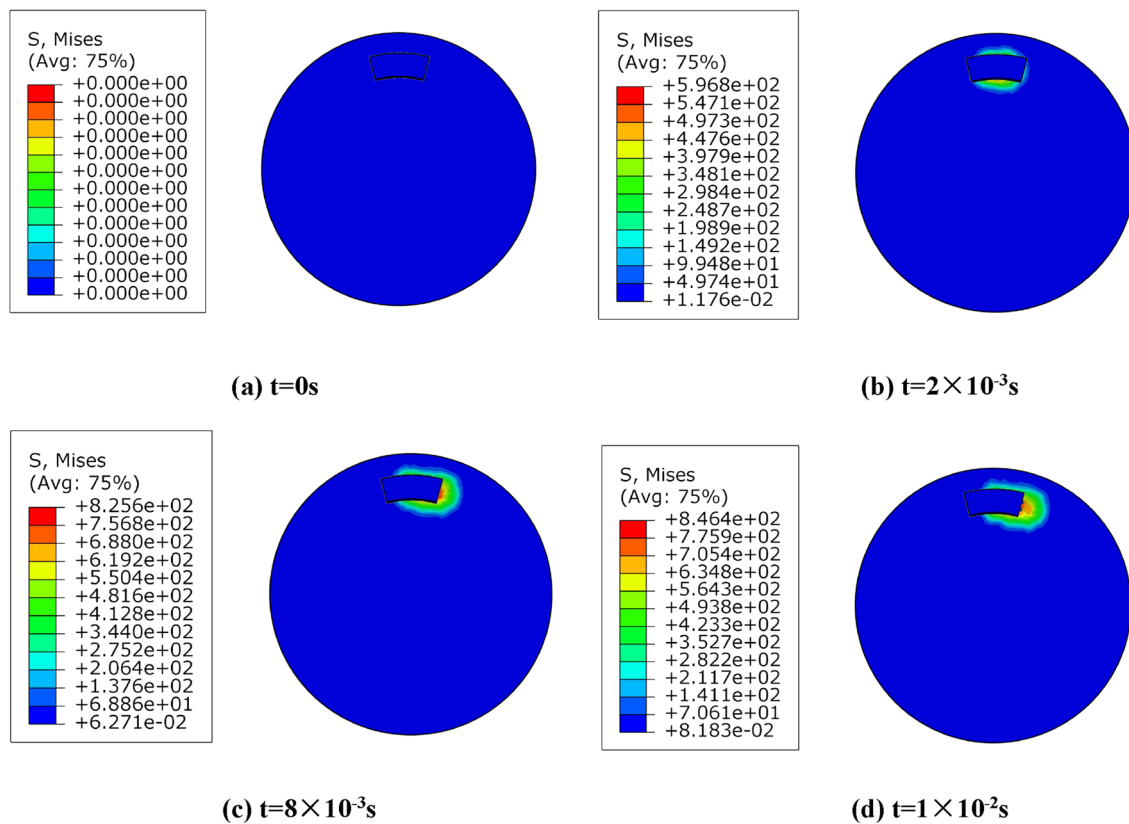


Fig. 6 The process of movement under different moments

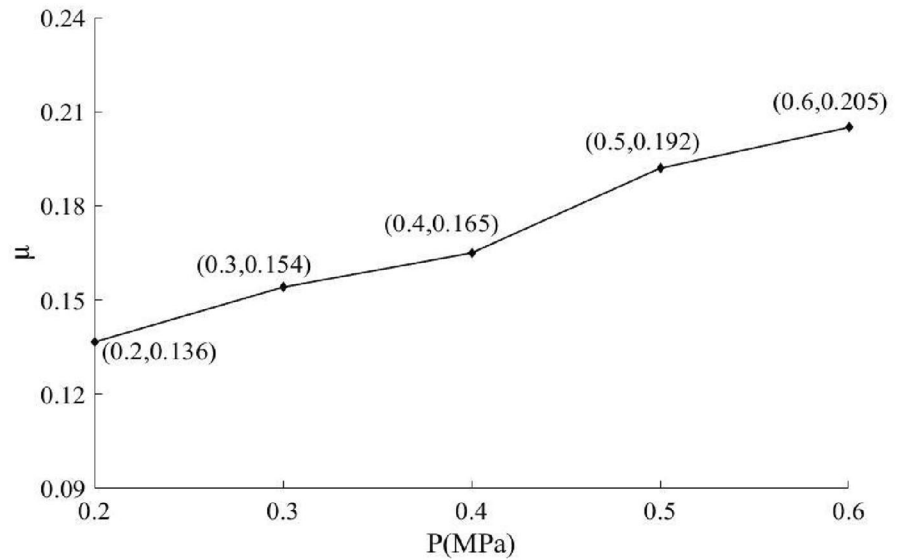
surface roughness, the upper sample are polished with the same 800 # fine sandpaper before each test. Start the testing machine, grind it for 3000 revolutions initially, so that the friction surfaces can be fully contacted, and then start the formal test at 5000 revolutions. The particles flow into the friction surface through a funnel that can control the outflow rate, as shown in Fig. 13c. Add weights and press the two friction blocks installed in the clamping slot of the fixture on the working surface of the friction disc through the pressing device. The test piece and the friction disc have a certain contact pressure. When the spindle drives the brake disc to rotate, it can create a frictional force tangential to the contact surface. The friction force causes the side force spring in the force measuring device to be deformed by the tensile force. The value of the friction force can be obtained by multiplying the deformation amount by the stiffness of the force measuring spring, and then dividing it by the corresponding positive pressure is the friction coefficient. When a formal test cycle was completed, the average coefficient of friction (COF) and standard deviation (SD) were calculated for the post 2500 rpm stabilization phase, and each set of experiments needed to be repeated three times and averaged to exclude the influence of chance factors on the experimental findings.

Table 4 Numerical simulation results for three grid types

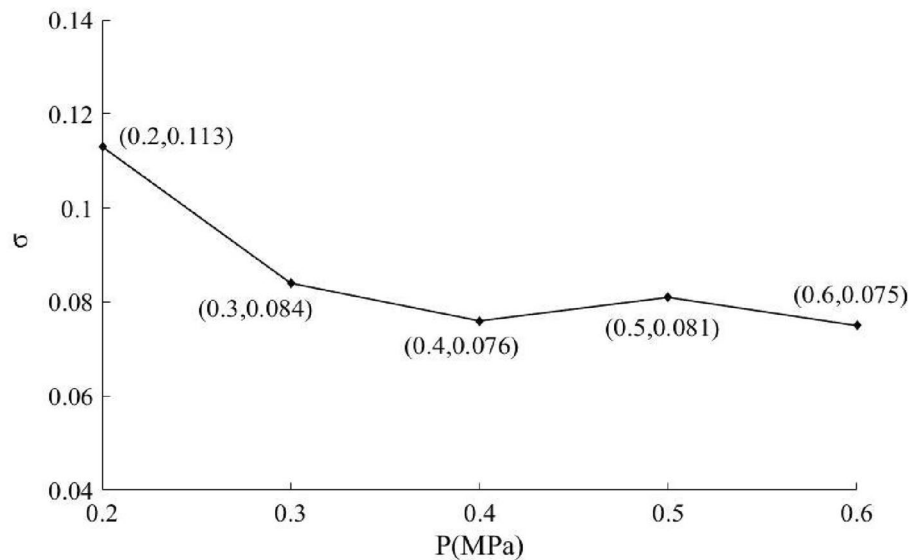
Mesh type	No. of elements	No. of nodes	Macroscopic friction coefficient	
			Min	Max
Coarse	3364	5116	0	0.334
Comparatively fine	8872	15,946	0	0.295
Fine	36,459	53,072	0	0.278

During the experiment to explore the effect of braking load on the friction performance of the three-body brake pair, the same amount of particles with a particle size of 30 μm were added to obtain the average friction coefficient and standard deviation under different braking pressures (367.5, 612.5, 857.5 and 1102.5 N), as shown in Fig. 14, it can be seen that the friction coefficient has a gradually increasing trend with the increase of the braking load. Abdul Hamid MK [11] did a similar study using abrasive particles from the environment and showed that the COF value also increases with increasing applied load.

Fig. 7 Influence of brake pressure on macroscopic friction coefficient of brake pair



(a) The variation of μ with P



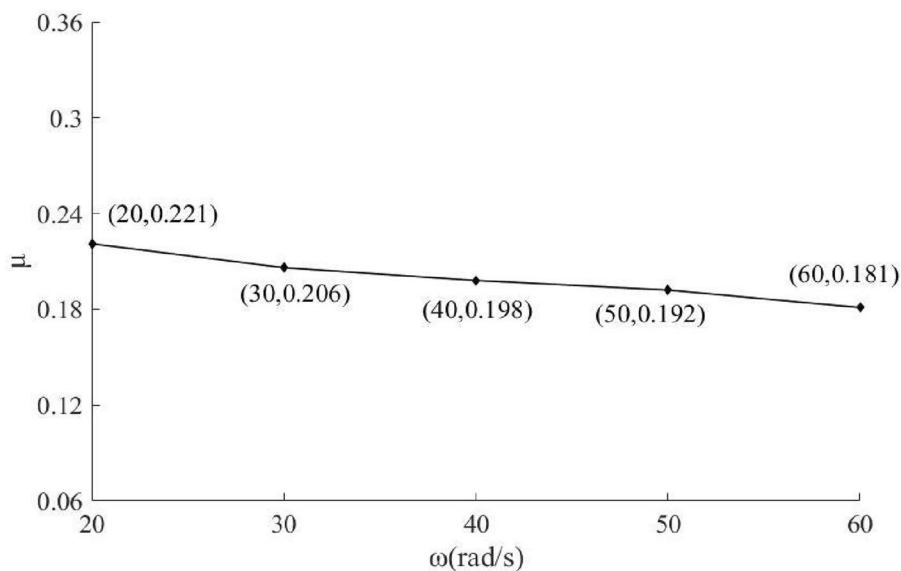
(b) The variation of σ with P

Particle Size Test

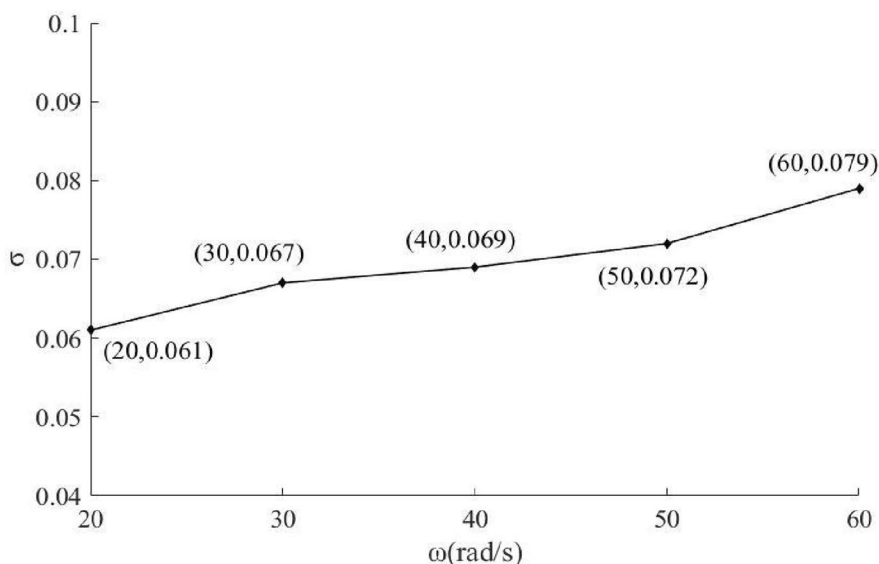
In the test process of investigating the influence of particle size on the friction performance of the three-body brake pair, the abrasive samples from the particle-free experimental process were collected, and the morphology is shown in Fig. 15a, and tested by MS-2000 laser particle size analyzer at the Analysis and Testing Center of Hefei University of Technology, where the horizontal coordinates in Fig. 15b is the particle size (μm) and the vertical coordinate is the volume specific gravity (%), and the average particle size is $5.763 \mu\text{m}$, which can verify the particle size and reduce

the experimental error. The same XD-MSM constant speeds friction tester was used to obtain COF and SD for different particle sizes (0, 30, 60, 90 and $180 \mu\text{m}$) by keeping the load constant, and the results are shown in Fig. 16, which shows that the friction coefficient tends to decrease gradually with the increase of particle size. Abdul Hamid MK [11] also concluded that the presence of abrasive particles has a significant effect on the COF values. The COF values tend to decrease when abrasive grains are present and increase as the size of abrasive grains decreases.

Fig. 8 Influence of angular velocity of brake disc on macroscopic friction coefficient of brake pair



(a) The variation of μ with ω



(b) The variation of σ with ω

Macroscopic Friction Coefficient Modeling

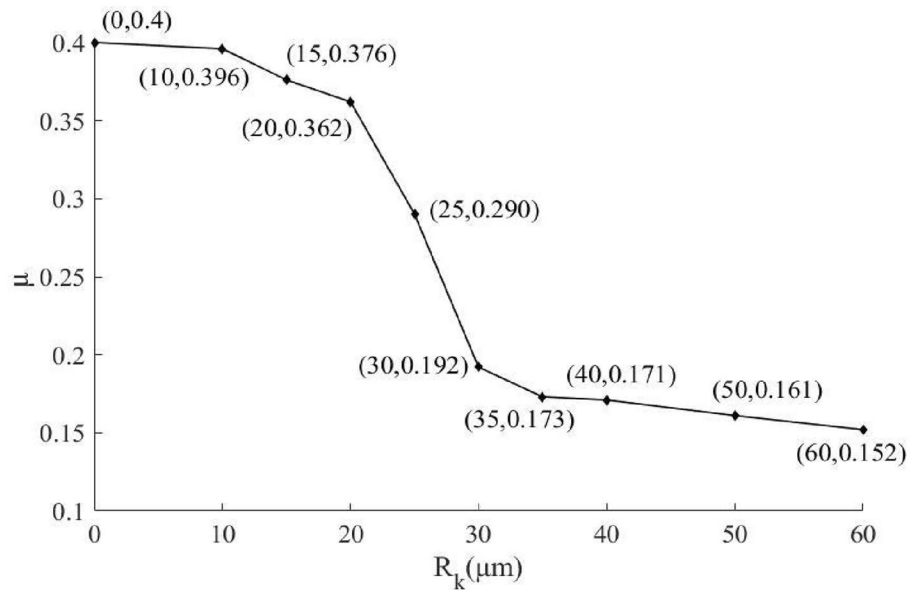
Derivation of Macroscopic Friction Coefficient Model

During the friction process, the frictional characteristics of the braking system change along with various physical and chemical changes and energy transformations on the friction surface. Ostermeyer et al. [26, 27] established a first order differential equation to study the dynamic characteristics of the brake pair friction, the idea of which is shown in Eq. (3) [27]:

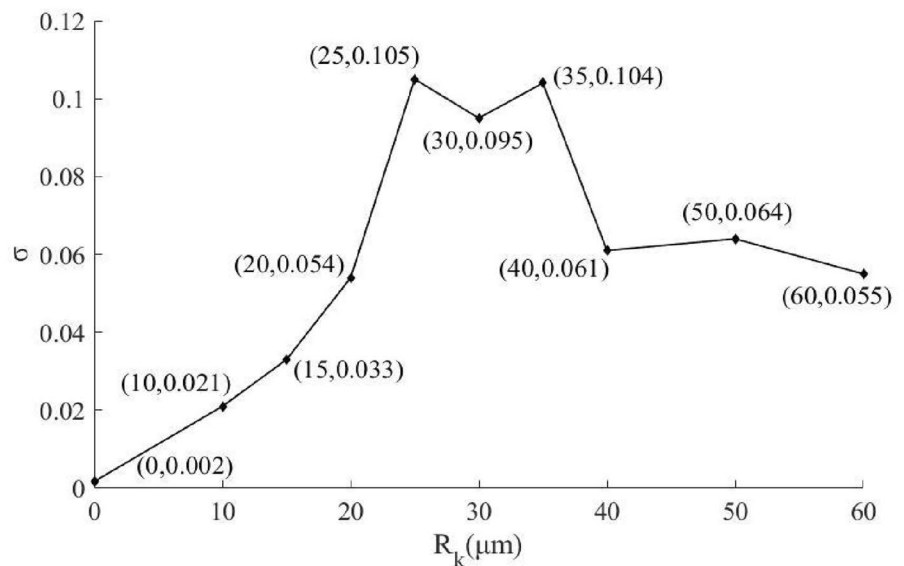
$$\begin{cases} \dot{\mu} = f(\mu, \text{var}_1, \text{var}_2, \dots) - g(\mu, \text{var}_1, \text{var}_2, \dots) \\ \text{var}_1 = f_1(\mu, \text{var}_1, \text{var}_2, \dots) - g_1(\mu, \text{var}_1, \text{var}_2, \dots) \\ \text{var}_2 = f_2(\mu, \text{var}_1, \text{var}_2, \dots) - g_2(\mu, \text{var}_1, \text{var}_2, \dots) \\ \vdots \end{cases} \quad (3)$$

In Eq. (3), $\text{var}_i (i = 1, 2, \dots)$ is the parameter affecting the friction characteristics of the braking pair, such as braking pressure, braking speed, and wear amount. $\dot{\mu}$ and var_i represent the friction coefficient and the rate of change of various characteristic parameters with time, whose

Fig. 9 Influence of particle size on macroscopic friction coefficient of brake pair



(a) The variation of μ with R_k

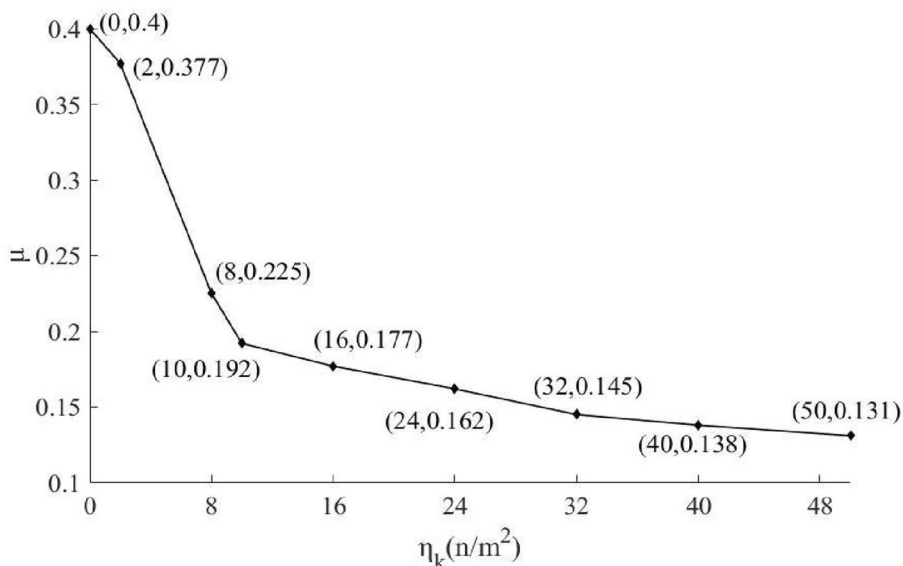


(b) The variation of σ with R_k

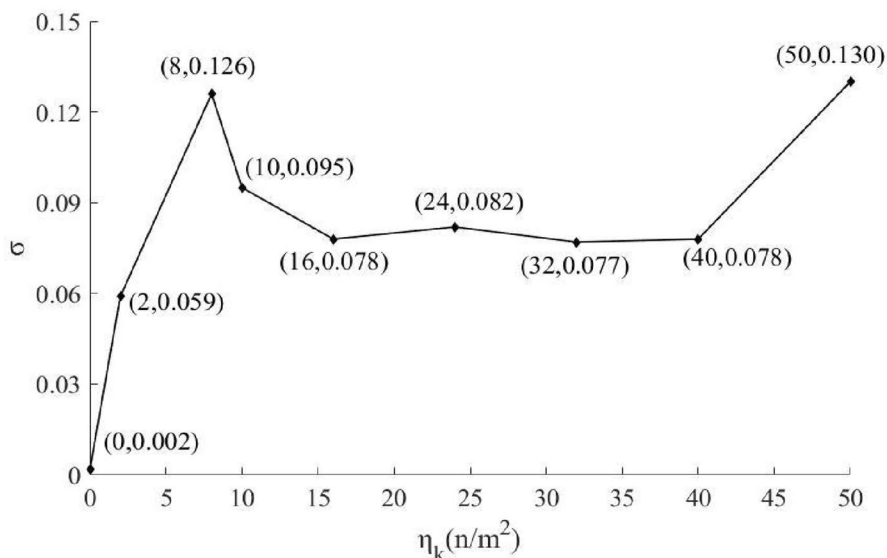
expressions are represented by the system variables. The expression on the right side of the equation is divided into two parts, where function f, f_1, f_2, \dots represents the influencing factors that make the friction coefficient and characteristic parameters increase, while function g, g_1, g_2, \dots represents the influencing factors that make the friction coefficient and characteristic parameters decrease. As can be seen, the model can take into account any factor of interest by simply changing the expression at the right end of the equation, and the key to the model is to construct functions that affect the friction coefficient and the characteristic parameters.

It can be seen from the analysis of the simulation data that the third body particles have a non-negligible effect on the friction performance of the brake pair. To accurately describe the friction performance of the braking pair, it is necessary to consider the third-body particles and the parameters of the braking interface. Starting from the factors that affect the actual contact area, the factors that affect the macroscopic friction coefficient are taken into account in the expression. In the process of friction, the actual contact area is composed of a two-body area and a three-body area. When the particle size is large enough and the number is large enough, the contact state of the brake disc surface at

Fig. 10 Influence of particle density on friction performance of brake pair



(a) The variation of μ with η_k



(b) The variation of σ with η_k

this time can be regarded as direct contact with the particle surface, if the initial actual contact area is larger, the more particle contact action, so from this perspective, the angular velocity of the brake disc, particle size, particle density and the actual contact area play a weakening effect on the macro friction coefficient, which can be expressed as a function *g*:

$$g = a_1\omega + a_2R_k + a_3\eta_k + a_4\frac{A_c}{A_p}, \tag{4}$$

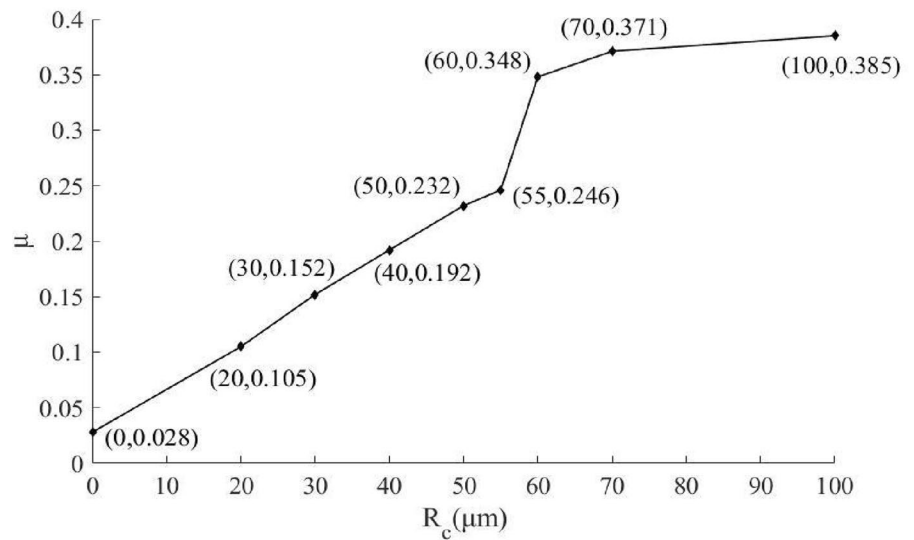
where *A_c* and *A_p* are the actual and nominal contact area of the brake block, respectively, *a₁*, *a₂*, *a₃* and *a₄* are coefficients

to be determined. From another point of view, with the increase of braking pressure and the radius of the rough peak of the brake block, a large number of particles occur embedded. At this time the contact state of the brake disc surface can be regarded as direct contact with the surface of the brake block, so it can be expressed as a function *f*:

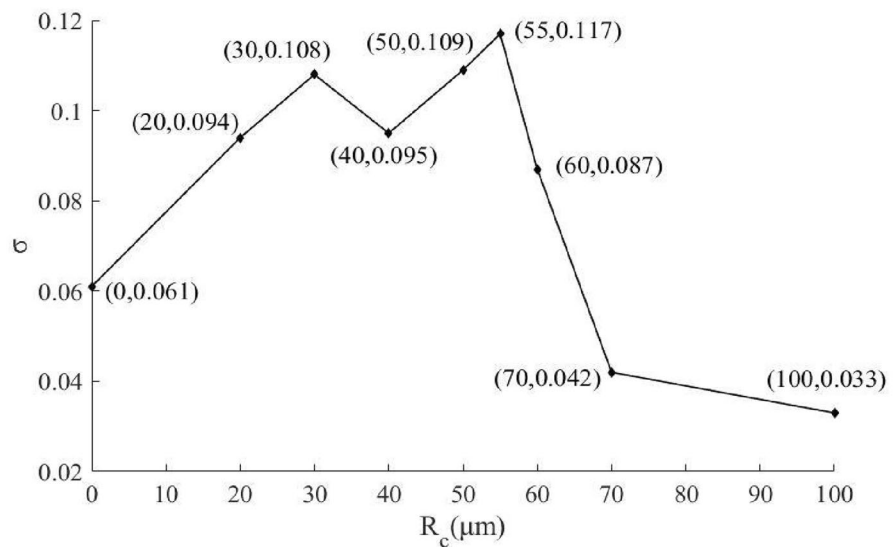
$$f = a_5P + a_6R_c, \tag{5}$$

where *a₅* and *a₆* are coefficients to be determined. From Eq. (5), the numerator denominator of the macroscopic friction coefficient is multiplied by the same *V_r* to obtain [27]:

Fig. 11 Influence of rough peak radius of brake block on macroscopic friction coefficient of brake pair



(a) The variation of μ with R_c



(b) The variation of σ with R_c

$$\mu = \frac{F_f V_r}{F_n V_r} \tag{6}$$

In Eq. (6), $F_f V_r$ is called the frictional power and $F_n V_r$ is called the inert power, which shows that the macroscopic friction coefficient is proportional to the frictional power, and the magnitude of the frictional power is also proportional to the real contact area. Therefore, to simplify Eq. (4), the relationship between the macroscopic friction coefficient and the real contact area can be expressed as [27]:

$$\mu = a_7 \frac{A_c}{A_p} \tag{7}$$

where a_7 is the coefficient to be determined. Bringing Eq. (7) into Eq. (4), we get:

$$g = a_1 \omega + a_2 R_k + a_3 \eta_k + \frac{a_4}{a_7} \mu \tag{8}$$

At this point, the differential equation for the macroscopic friction coefficient can be expressed as

$$\dot{\mu} = a_5 P + a_6 R_c - a_1 \omega - a_2 R_k - a_3 \eta_k - \frac{a_4}{a_7} \mu \tag{9}$$

Define the coefficients $a = a_5$, $b = a_6$, $c = a_1$, $d = a_2$, $e = a_3$, $f = \frac{a_4}{a_7}$, then

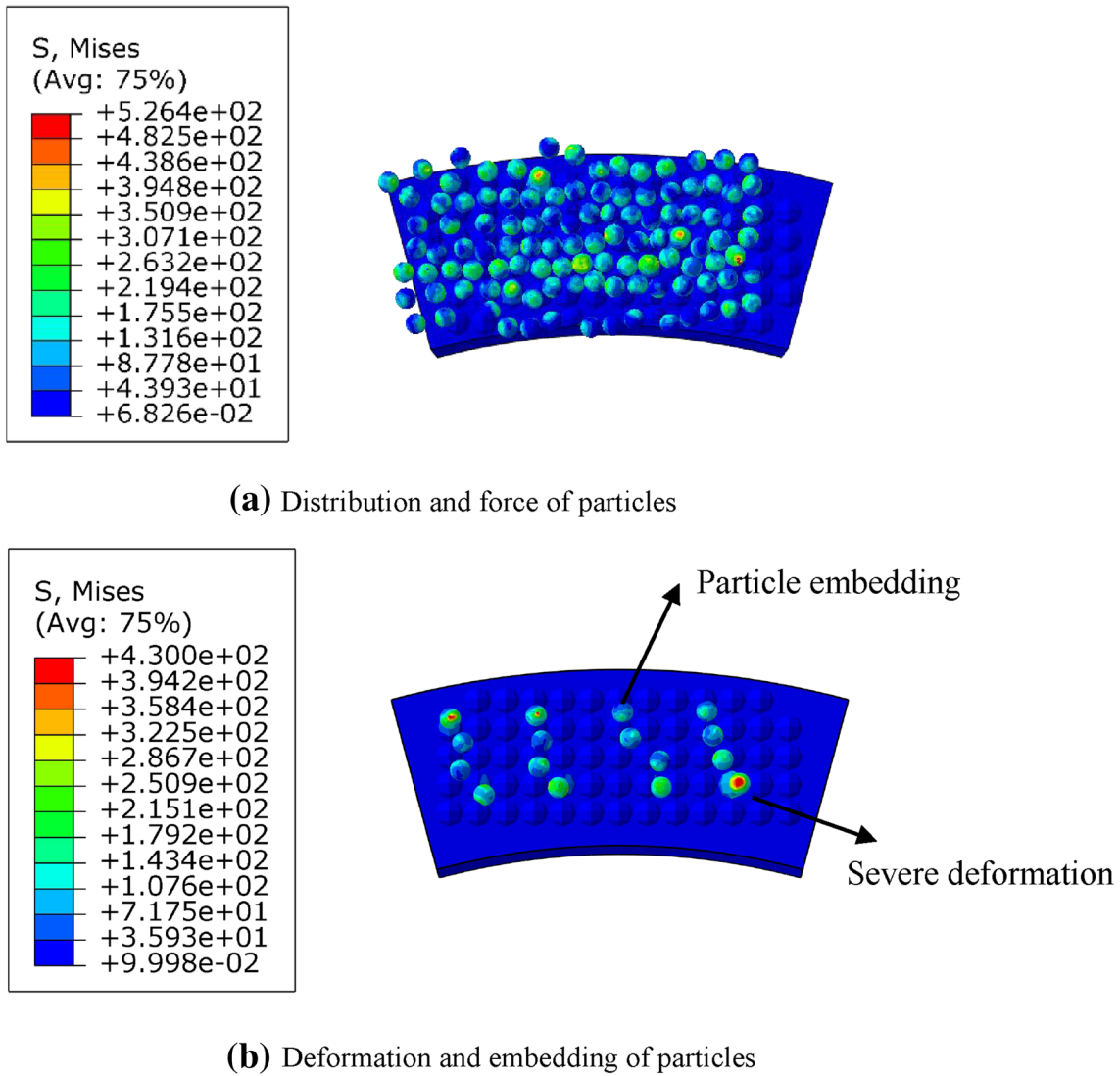


Fig. 12 The motion state of the third body particles during braking

$$\dot{\mu} = aP + bR_c - c\omega - dR_k - e\eta_k - f\mu. \tag{10}$$

Equation (10) is the established differential equation. In the formula, a, b, c, d, e and f are undetermined coefficients, which can be determined by simulation data. The general solution of this differential equation is of the following form:

$$\mu(t) = \frac{-(-aP - bR_c + cW + dR_k + eR_k + C_1 e^{-ft})}{f}, \tag{11}$$

where C_1 is a coefficient to be determined by the initial conditions. When time tends to infinity, the steady-state macroscopic friction coefficient μ_{stab} can be obtained, and its expression is

$$\mu_{stab} = \frac{aP + bR_c - c\omega - dR_k - eR_k}{f}. \tag{12}$$

The settings of the key braking parameters of brake pressure, angular velocity of the brake disc, particle size, particle density and rough peak radius of the brake block were changed in ABAQUS to obtain a large number of simulation data of steady-state macroscopic friction coefficients under different conditions, and multiple regression analysis was performed on the data to calculate the coefficients to be determined as shown in Table 5.



Fig. 13 XD-MSM constant speed friction tester

Prediction of Regression Analysis Results

1. Prediction of steady-state macroscopic friction coefficient under single parameter variation

Using Eq. (12) to predict the steady-state macroscopic friction coefficient for different single parameter variations, the results were compared with the finite element simulation results and the SSE and R-square values of the model were calculated, and the results are shown in Fig. 17. It can be seen that the values of the steady-state macroscopic friction coefficient predicted with Eq. (12) are very close to the simulated values with R-square values above 0.9 for a single parameter change, indicating that the model is relatively accurate in predicting the steady-state macroscopic friction coefficient under a single parameter change.

2. Prediction of steady-state macroscopic friction coefficients under multiple parameter variations

The formula obtained by regression analysis is used to predict the steady-state macroscopic friction coefficient under multiple parameter changes, and the comparison with the finite element simulation results is shown in Table 6. From the results in the table, the simulated values

are in good agreement with the predicted values under multiple parameter changes, indicating that the relationship between the steady-state macroscopic friction coefficient and the key braking parameters is relatively accurate.

Conclusion

This paper first establishes the three-dimensional model of disc brake pair, and explores the macroscopic friction coefficient and friction stability under different braking conditions by changing the braking pressure, angular velocity of the brake disc, particle size, particle density and rough peak radius of the brake block, and analyzes the change mechanism, and verifies the simulation results using bench experiments. Finally, the macroscopic friction coefficient model was established and the following conclusions were drawn:

1. When the third body particles are added to the brake interface, it will significantly affect the friction performance of the brake pair. As the particle size increases, the macroscopic friction coefficient tends to decrease, from 0.4 to 0.152. As the particle density increases, the

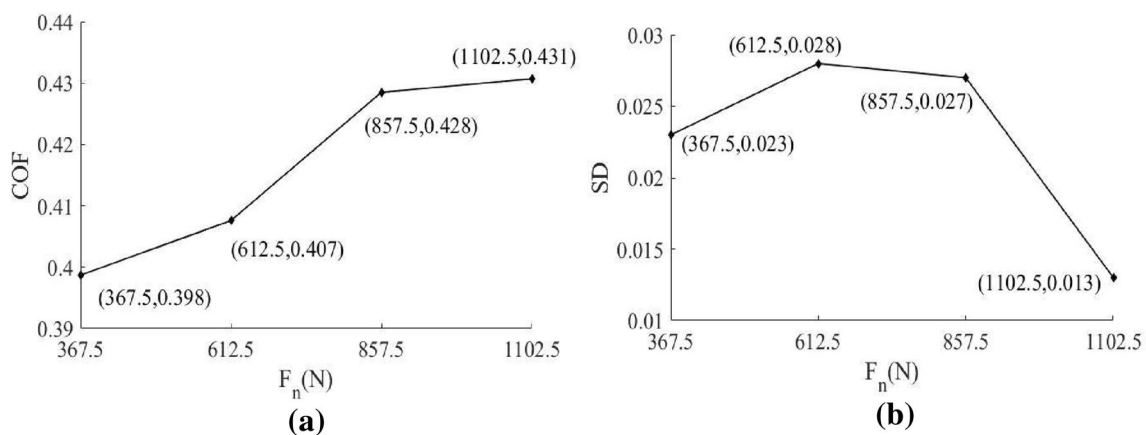
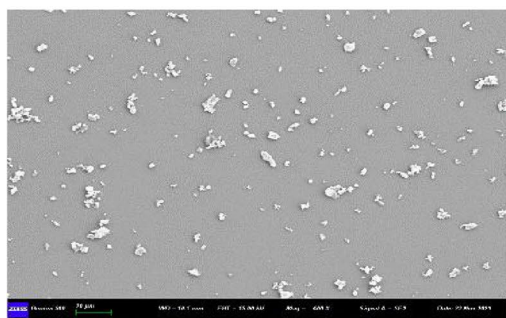
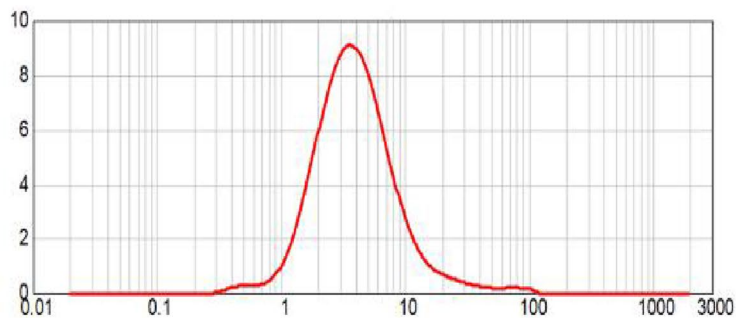


Fig. 14 Experimental results on the effect of braking load on the frictional performance of three-body brake pair



(a) Abrasive chip shape



(b) Abrasive chip size distribution

Fig. 15 Abrasive chip sample analysis

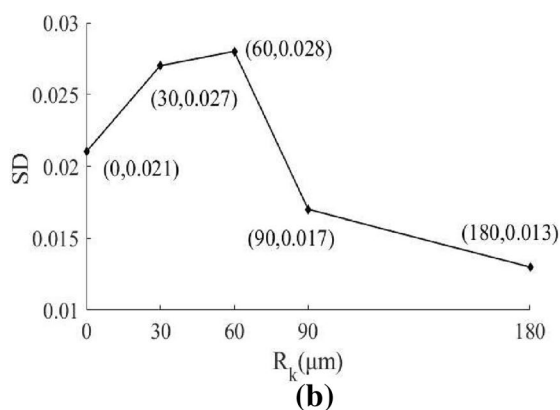
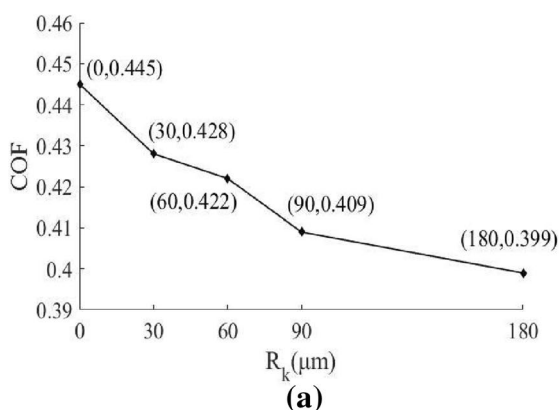


Fig. 16 Experimental results on the effect of particle size on the frictional performance of three-body brake pair

macroscopic friction coefficient tends to decrease, from 0.4 to 0.131. As the rough peak radius of the brake block increases, the macroscopic friction coefficient tends to increase, from 0.028 to 0.385.

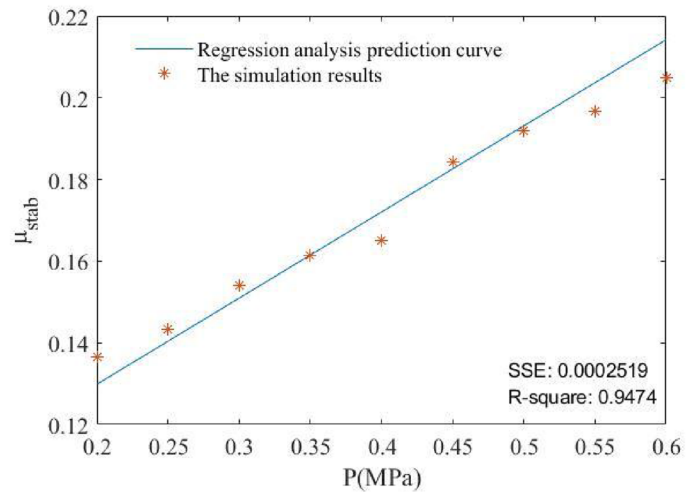
- Through the research on the matching relationship between particle size and the surface roughness peak of the brake block, it is found that the macroscopic friction coefficient increases gradually with the increase of the ratio of the rough peak radius of the brake block to the particle size. When the size ratio is about 1.5, the friction coefficient. The coefficient changes most drastically, which can provide a theoretical reference for the design of the brake block to achieve the best braking performance.
- Braking parameters affect the friction performance of the braking pair by changing the deformation and embedding of the particles. Higher braking pressure increases the degree of particle deformation and increases the proportion of particles embedded in the rough crest gap of

the brake block, both of which increase the macroscopic friction coefficient. The increase of the angular velocity of the brake disc will speed up the flow of the particles, but it is not easy to fall into the gap between the rough peaks, and the macroscopic friction coefficient decreases slowly. The larger the particle size, the stronger the load-bearing deformation capacity, and the less likely to be embedded, resulting in a decrease in the macroscopic friction coefficient. As the density of particles in the brake interface increases, the average load on each particle is lower, the deformation is weaker, the rolling friction component is higher, and the macroscopic friction coefficient becomes smaller. And the larger the radius of the rough peak of the brake block, the easier the particles are embedded in the rough peak gap of the brake

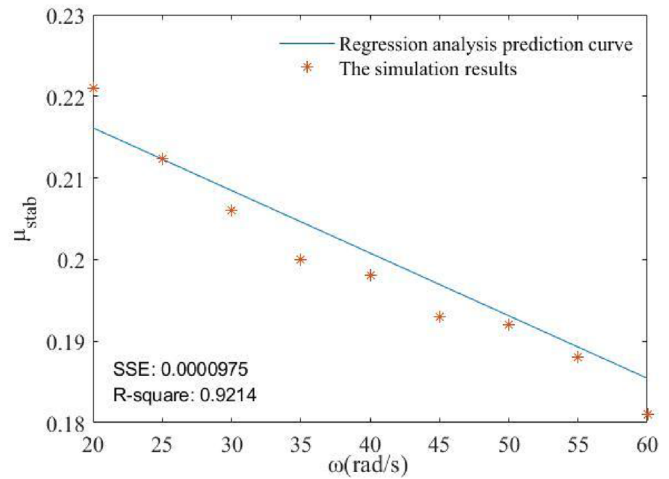
Table 5 Calculation result of undetermined coefficient

<i>a</i>	<i>b</i>	<i>c</i>	<i>d</i>	<i>e</i>	<i>f</i>
0.190519	0.004074	0.000693	0.001065	0.001722	0.903065

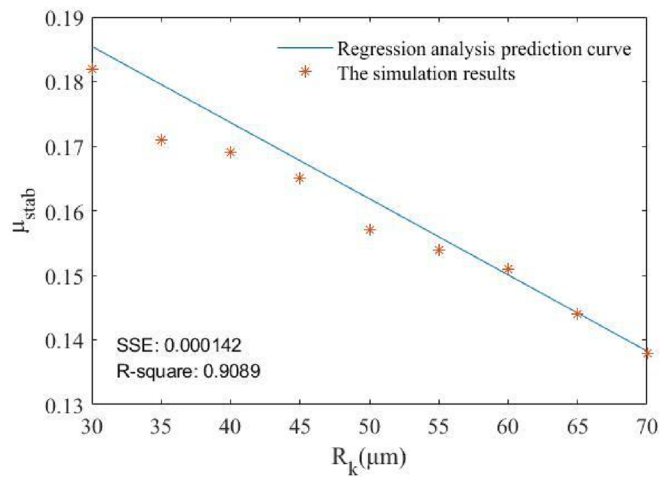
Fig. 17 Comparison between the predicted value of the steady-state friction coefficient model established under different parameter changes and the simulation results



(a) $\omega=50$ rad/s, $R_k=30$ μm , $R_c=40$ μm , $\eta_k=10$ /m²

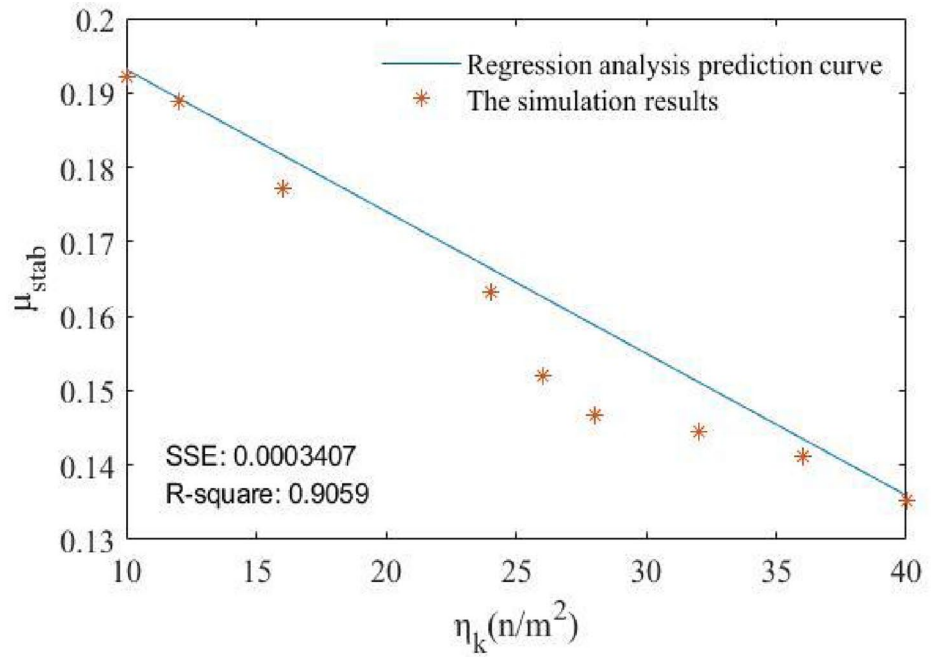


(b) $P=0.5$ MPa, $R_k=30$ μm , $R_c=40$ μm , $\eta_k=10$ /m²

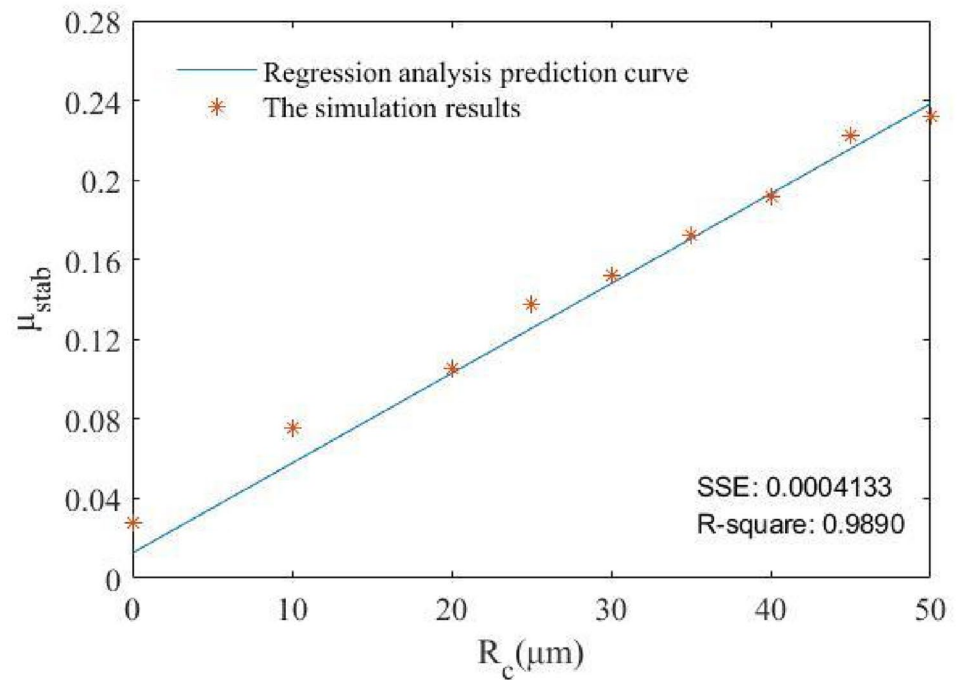


(c) $\omega=60$ rad/s, $P=0.5$ MPa, $R_c=40$ μm , $\eta_k=10$ /m²

Fig. 17 (continued)



(d) $\omega=50$ rad/s, $R_k=30$ μm , $R_c=40$ μm , $P=0.5$ MPa



(e) $\omega=50$ rad/s, $R_k=30$ μm , $\eta_k=10$ / m^2 , $P=0.5$ MPa

block, so the macroscopic friction coefficient increases and fluctuates less.

4. Drawing on the idea of Ostermeyer's model [27], a macroscopic friction coefficient model considering the third-

Table 6 Steady-state macroscopic friction coefficient under multiple parameter variations

The serial number	1	2	3	4
Brake pressure, P (MPa)	0.55	0.44	0.49	0.58
Brake disc angular velocity, ω (rad/s)	45	42	52	34
Particle size, R_k (μm)	28	32	40	22
Particle density, η_k (n/m^2)	8	13	11	9
Rough peak radius of brake block, R_c (μm)	32	45	42	38
The simulation value of μ_{stab}	0.1809	0.1931	0.1591	0.2158
The predicted value of μ_{stab}	0.1775	0.2011	0.1685	0.2246

body particles and interface parameters was established, and the coefficients were determined by multiple regression analysis to calculate the steady-state macroscopic friction coefficients under different braking key parameters, and the R-square values of the models were above 0.9, which basically matched with the simulation results to verify the reliability of the proposed friction model.

The effect of temperature on the friction characteristics of the brake pair interface is not considered during the simulation in this paper. In the actual braking process, the disc block surface often has a higher temperature, which will affect the stress–strain at the contact interface and thus the value of the friction coefficient, so future simulation modeling can consider the effect of temperature.

Acknowledgements This project is supported by National Natural Science Foundation of China (Grant no. 51875154) and Wuhu Applied Basic Research Project (Grant No. 2022jc03).

References

- Sakuma H, Kawai K, Katayama I et al (2018) What is the origin of macroscopic friction? [J]. *Sci Adv* 4(12):1–5
- Liew KW, Nirmal U (2013) Frictional performance evaluation of newly designed brake pad materials. *Mater Des* 48(1):25–33
- Eriksson M, Bergman F, Jacobson S (2002) On the nature of tribological contact in automotive brakes. *Wear* 252(1–2):26–36
- Jang H, Lee JS, Fash JW (2001) Compositional effects of the brake friction material on creep groan phenomena. *Wear* 251(1–12):1477–1483
- Wagner UV, Hochlenert D, Hagedorn P (2007) Minimal models for disk brake squeal. *J Sound Vib* 302(3):527–539
- Godet M (1984) The third-body approach: a mechanical view of wear. *Wear* 100(1–3):437–452
- Kchaou M, Lazim AM, Hamid MA, Bakar AA (2017) Experimental studies of friction-induced brake squeal: influence of environmental sand particles in the interface brake pad-disc. *Tribol Int* 110:307–317
- Sun W, Zhou W, Liu J, Fu X, Chen G, Yao S (2018) The size effect of SiO_2 particles on friction mechanisms of a composite friction material. *Tribol Lett* 66(1):35
- Sterle W, Drfel I, Prietzel C, Roach H, Desplanques Y (2009) A comprehensive microscopic study of third body formation at the interface between a brake pad and brake disc during the final stage of a pin-on-disc test. *Wear* 267(5):781–788
- Stojanovic N, Glisovic J, Abdullah OI et al (2022) Particle formation due to brake wear, influence on the people health and measures for their reduction: a review [J]. *Environ Sci Pollut Res* 29(7):9606–9625
- Abdul Hamid MK (2010) Study of the grit particle size and shape effects on the frictional characteristics of the automotive braking system. *Adv Mater* 189–193:3511
- Desplanques Y, Degallaix G (2008) Interactions between third-body flows and localisation phenomena during railway high-energy stop braking. *Sae Int J Passeng Cars Mech Syst* 1(1):1267–1275
- Cho KH, Jang H, Hong YS, Kim SJ, Fash JW (2008) The size effect of zircon particles on the friction characteristics of brake lining materials. *Wear* 264(3–4):291–297
- Hamid MA, Stachowiak GW (2011) The effects of grit particle size on frictional characteristics of automotive braking system. *Adv Mater Res* 189–193:3511–3516
- Belhocine A, Abdullah OI (2020) Finite element analysis (FEA) of frictional contact phenomenon on vehicle braking system [J]. *Mech Based Des Struct Mach* 2:1–36
- Belhocine A, Abdullah OI (2020) Thermomechanical model for the analysis of disc brake using the finite element method in frictional contact (Multiscale Science and Engineering ISSN 2524–4515)
- Belhocine A, Abdullah OI (2020) A thermomechanical model for the analysis of disc brake using the finite element method in frictional contact [J]. *J Therm Stress* 43(3):305–320
- Belhocine A, Omar WZW (2016) Three-dimensional finite element modeling and analysis of the mechanical behavior of dry contact slipping between the disc and the brake pads [J]. *Int J Adv Manuf Technol*
- Belhocine A, Ghazaly NM (2016) Effects of Young's modulus on disc brake squeal using finite element analysis [J]. *Int J Acoust Vib* 21(3):292–300
- Iordanoff I, Berthier Y, Descartes S et al (2002) A review of recent approaches for modeling solid third bodies [J]. *J Tribol* 124(4):725–735
- Fillot N, Iordanoff I, Berthier Y (2005) Simulation of wear through mass balance in a dry contact [C]. In: *Asme/stle international joint tribology conference*
- Hou SQ, Wang W, Wang ZY et al (2018) Force chain characteristics and effects of a dense granular flow system in a third body interface during the shear dilatancy process [J]. *J Appl Mech Tech Phys* 59(1):153–162
- Shuqing H (2018) Characterization of the non-stationary behavior of confined granular bodies in micro-regions at friction interfaces [D]. Hefei University of Technology
- Huang T, Wei D, Zhu Y et al (2022) The establishment and dynamic analysis of a new friction model of brake pair considering interface morphology and particles. *Proc Inst Mech Eng Part C J Mech Eng Sci* 236(9):4988–5004

25. Peng T, Yan Q, Li G, Zhang X, Wen Z, Jin X (2017) The braking behaviors of Cu-based metallic brake pad for high-speed train under different initial braking speed. *Tribol Lett* 65(4):1–13
26. Ostermeyer GP (2003) On the dynamics of the friction coefficient[J]. *Wear* 254(9):852–858
27. Ostermeyer GP, Müller M (2008) New insights into the tribology of brake systems [J]. *Proc Inst Mech Eng Part D J Automob Eng* 222(7):1167–1200

Publisher's Note Springer Nature remains neutral with regard to jurisdictional claims in published maps and institutional affiliations.

Springer Nature or its licensor (e.g. a society or other partner) holds exclusive rights to this article under a publishing agreement with the author(s) or other rightsholder(s); author self-archiving of the accepted manuscript version of this article is solely governed by the terms of such publishing agreement and applicable law.